

Parametric x-radiation in a mosaic crystal of pyrolytic

K. Yu. Amosov, M. Yu. Andreyashkin, V. A. Verzilov, I. E. Vnukov,
V. N. Zabaev, B. N. Kalinin, V. V. Kaplin, D. V. Kustov, G. A. Naumenko,
Yu. L. Pivovarov, A. P. Potylitsyn, E. I. Rozum, and S. R. Uglov

*Scientific-Research Institute of Nuclear Physics, Tomsk Polytechnical University,
634050 Tomsk Box 25, Russia*

M. Moran

Lawrence Livermore National Laboratory, Livermore, California 94550, US

(Submitted 29 August 1994)

Pis'ma Zh. Eksp. Teor. Fiz. **60**, No. 7, 506–510 (10 October 1994)

Anomalously high orders of parametric x-radiation of 900-MeV electrons in a crystal of pyrolytic graphite have been observed experimentally at the Tomsk synchrotron. This observation supports results found by Fiorito *et al.* [Phys. Rev. Lett. **71**, 704 (1993)] at an electron energy of 90 MeV. The angular distributions of the photons in the peaks of the parametric x-radiation have been measured up to fourth order for the first time. The results are compared with the kinematic theory of parametric x-radiation. © 1994 American Institute of Physics.

The numerous experimental studies of the characteristics of parametric x-radiation (PXR) have generally used high-quality single-crystal targets (of Si, Ge, natural diamond, and quartz), with a mosaic spread no greater than^{1–4} 0.2 mrad. Comparison of the results with the theory has revealed a good agreement with calculations from the kinematic model.^{5,6} The first experiment on the generation of PXR in mosaic pyrolytic graphite was carried out by Fiorito *et al.*⁷ The results showed that (first) very high orders (up to $n=8$) are observed in the emission spectrum and (second) the intensity ratio of the emission of PXR of high orders to the first order is not described by the model of Ref. 5, which deals with the effects of the beam divergence and the mosaic structure in a phenomenological way. Rule *et al.*⁸ have proposed a method for calculating the PXR spectrum for mosaic crystals. Potylitsyn⁹ has proposed a way to deal with the effect of the mosaic structure on the angular distributions of the PXR.

Unfortunately, no data on the absolute intensity of the PXR for pyrolytic graphite were reported in Ref. 7; it is thus difficult to make a comparison with theory. The relation between PXR and the diffraction of real bremsstrahlung photons remains an open question.

In this paper we are reporting measurements of the intensity of PXR per electron with the help of pyrolytic graphite prepared by the technology developed at Union Carbide, i.e., using the same technology used for the target in the experiments of Ref. 7. Measurements were carried out for an electron energy $E_e=900$ MeV, at which the diffraction of real bremsstrahlung photons clearly makes only a small contribution.

The experiment was carried out on the inner beam of the Sirius synchrotron in the Bragg geometry: The angle between the momentum of an electron and the (200) crystal

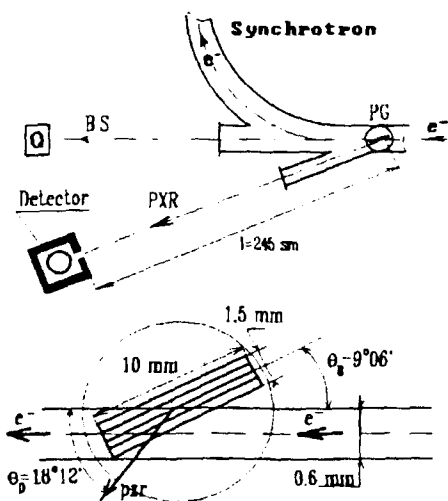


FIG. 1. Experimental layout.

crystallographic planes was $\theta_B = 9^\circ 06'$; the angle between the electron momentum and a photon of the PXR was $\theta_D = 18^\circ 12'$ (Fig. 1). The energy of the electron beam was $E_e = 900 \pm 5$ MeV, the divergence was $\Delta\theta_e \approx 0.1$ mrad, and the duration of the dump was $\Delta t = 12$ ms. The angle θ_B was reckoned from the “physical” zero, which was determined from the emission in the case of channeling when the (200) planes of graphite coincided with the direction of the electron momentum. The emission during channeling was detected directly ahead of the ionization chamber (Fig. 1a).

The graphite crystal used in the experiments had dimensions of $10 \times 6 \times 1.5$ mm. Because of the large dimensions of this crystal (10 mm in the direction along the beam) and the comparatively small angle at which the photons are emitted, there is the problem of dealing correctly with the absorption of PXR photons in the target. To simplify this problem we used an electron beam with a transverse dimension $\Delta r = 0.6 \pm 0.1$ mm, which interacted with only part of the target (Fig. 1b). The transverse dimension of the beam was adjusted with a “scraper” at an azimuthal angle of 180° from the target.¹⁰ The transverse dimension of the beam was monitored by measuring the PXR intensity as a function of the position of the scraper. For the geometry shown in Fig. 1b, the average target thickness \bar{t} is determined by the transverse dimension of the beam. It can be shown that for $\Delta r = 0.6$ mm the average thickness is $\bar{t} = 1.9$ mm; this is ≈ 0.01 of a radiation length. The calculated bremsstrahlung intensity for the given target thickness was used to estimate the number of electrons which passed through the target in measurements of the total energy of the bremsstrahlung beam by a Gauss quantometer.

The PXR was detected alternately by two detectors (Fig. 1(a): a) A BDP-2 xenon-filled proportional counter with an aperture of 4×16 mm and an efficiency $f = 60\%$ for a photon energy $\hbar\omega = 11$ keV or $f \approx 10\%$ for $\hbar\omega = 22$ keV. This counter could be moved in vertical and horizontal directions in order to find the center of a reflection of the PXR. b) A DGR5-1 germanium semiconductor detector with an aperture ≈ 150 mm² and a crystal thickness of 5 mm.

The experimental apparatus and the procedure for sampling data are described in

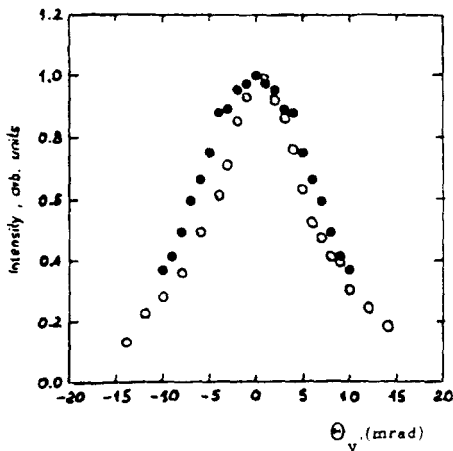


FIG. 2. Vertical distribution of the (200) reflection measured by the proportional counter. ○—Experimental; ●—Theoretical.

detail in Ref. 11. The resolution of the proportional counter at the Zn^{63} line (8.1 keV) is 20%, and that of the semiconductor detector is 18%. The intensity of the electron beam was held at 10^7 – 10^8 e^- /cycle in the course of an experiment. In this case the percentage of counts missed by the proportional counter, which was monitored in each cycle of the accelerator, did not exceed 15%.

Figure 2 shows a spectrum and a vertical distribution of the (200) reflection (reflection order $n=1$, photon energy $\hbar\omega_{(200)}=11.2$ keV) measured by the proportional counter. Photons with an energy of 11.2 ± 0.5 keV were detected in the measurements of the vertical distribution of the reflection.

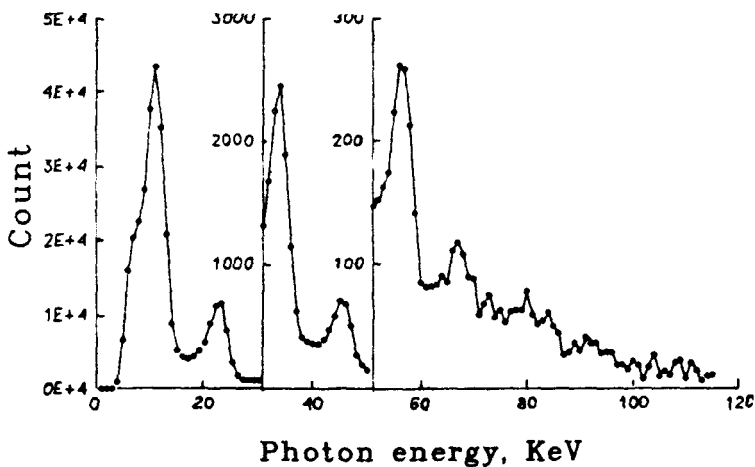


FIG. 3. Spectra of the parametric x radiation measured by the semiconductor detector. a—At the center of a reflection; b—at the edge of a reflection.

TABLE I.

	$dN_{(200)}/d\Omega$, photons/($e^- \cdot \text{sr}$)	$\Delta N_{(400)}/\Delta N_{(200)}$	$\Delta N_{(600)}/\Delta N_{(200)}$	$\Delta N_{(800)}/\Delta N_{(200)}$
Expt	0.46 ± 0.07	0.22 ± 0.04	0.026 ± 0.005	0.008 ± 0.0016
Theor	0.75	0.29	0.113	0.0494

The semiconductor detector was brought into coincidence with the center of the reflection within an error no greater than 3 mrad. The orientation of the crystal was then adjusted to bring the center of the reflection into coincidence with the detector in the horizontal plane also. Figure 3 shows a PXR spectrum measured by the semiconductor detector. We see that six orders of PXR, from (200) to (1200), are clearly present. To estimate a possible contribution from pulse overlap to the measured spectrum, we placed a copper filter 0.05 mm thick in front of the aperture of the semiconductor detector in a control measurement. This copper filter effectively cut out the first maximum of the PXR, while changing the second and subsequent reflections only negligibly. According to our estimates, the pulse overlap does not exceed 10% of the total count of the semiconductor detector. Table I shows the PXR brightness $dN/d\Omega$ as measured by the proportional counter for the (200) reflection. Also shown here are the brightnesses of all peaks after the first divided by the brightness of the first. These ratios were measured with the semiconductor detector. Note that, within the experimental errors, the values found for $N_{(400)}/N_{(200)}$ by the two detectors are the same.

Figure 4 shows measurements of the orientation dependence of the PXR yield for two orders, for a fixed position of the semiconductor detector. To find these orientation curves we measured spectra for various orientations of the crystal, θ_B , and we deter-

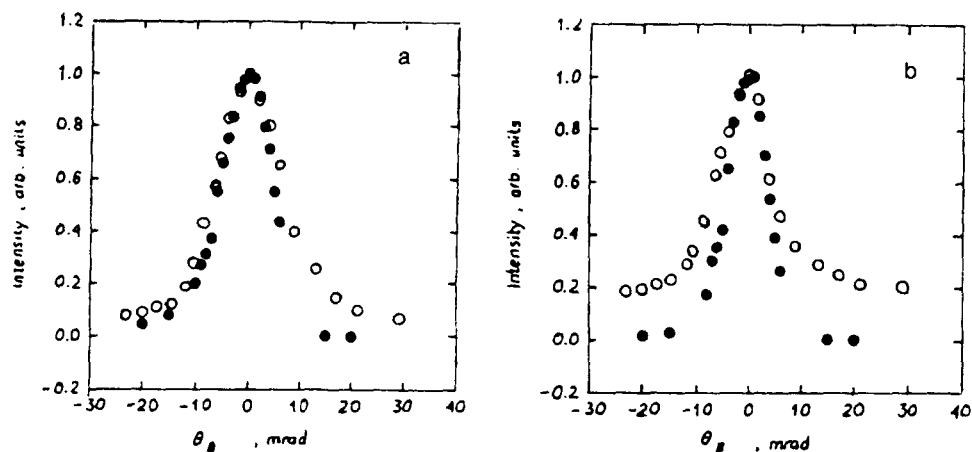


FIG. 4. Orientation curves for (a) the (200) reflection of parametric x radiation and (b) for the (800) reflection, measured by the semiconductor detector. \circ —Experimental; \bullet —theoretical.

TABLE II.

Order of reflection (<i>i</i>)		1	2	3	4
Theor	$\Delta\Theta_i$, mrad	11.8	10.0	9.6	8.9
	$\Delta\Theta_i / \Delta\Theta_1$,	1	0.847	0.81	0.754
Expt	$\Delta\Theta_i$, mrad	13.1 ± 0.6	10 ± 0.6	9.6 ± 0.6	8.9 ± 0.6
	$\Delta\Theta_i / \Delta\Theta_1$,	1	0.858	0.81	0.75

mined the number of photons in each peak after subtracting the continuous background. It follows from Fig. 4 that the orientation curves become narrower with increasing order of the reflection; the same effect is predicted by the theory of PXR. The results are summarized in Table II.

To make a comparison with the kinematic model of PXR, we calculated the measured curves for a Gaussian distribution of the mosaic structure of the graphite:

$$F_M(\alpha_x, \alpha_y) = \frac{1}{2\pi\sigma_M^2} \exp\left(-\frac{\alpha_x^2 + \alpha_y^2}{2\sigma_M^2}\right),$$

where α_x is the angular deviation of an element of the mosaic in the horizontal plane (the diffraction plane), and α_y is that in the vertical plane. We chose the standard deviation of the distribution to be $\sigma_M = 3.4$ mrad. We determined the angular distribution of the PXR reflection for a mosaic crystal in accordance with Ref. 9, after convolving the $F_M(\alpha_x, \alpha_y)$ spectrum with the angular distribution of the PXR. The yield of PXR photons into the fixed aperture of the detector for a given orientation of the crystal was found through a numerical integration of the resulting expression. The behavior calculated in this manner is shown in Figs. 2 and 4 and Tables I and II. In all cases, absorption in air and in the target material has been taken into account. Note that a satisfactory agreement is found for the angular distributions, while the yield of PXR for the higher reflections tends to fall below the theoretical value.

In conclusion we can point out the following: a) We have confirmed the result of Ref. 7, in which reflections of parametric x radiation of anomalously high orders were observed. We have measured the angular distributions of the photons in reflections up to fourth order of the PXR for the first time. b) The use of a comparatively thick, mosaic graphite target leads to a PXR yield significantly higher than that obtained from the thin crystals which have ordinarily been used. c) On the whole, the kinematic theory gives a satisfactory description of the angular distribution of the PXR reflections, while it is far less successful in describing the ratios of the PXR yields for the various orders. d) In order to make a correct comparison with the theory, it would be desirable to use mosaic targets with a known $F_M(\alpha_x, \alpha_y)$ distribution or carry out some independent measurements of the standard deviation σ_M .

¹Yu. N. Adishchev *et al.*, Zh. Eksp. Teor. Fiz. **93**, 1943 (1987) [Sov. Phys. JETP **66**, 1107 (1987)].

²S. Asano *et al.*, Phys. Rev. Lett. **70**, 3247 (1993).

³Yu. N. Adisheev *et al.*, Phys. Lett. A **147**, 326 (1990).

⁴A. R. Mkrtchyan *et al.*, Phys. Lett. A **152**, 297 (1991).

⁵I. D. Feranchuk and A. V. Ivashin, J. Phys. (Paris) **46**, 1981 (1985).

⁶H. Nitta, Phys. Lett. A **158**, 270 (1991).

⁷R. B. Fiorito *et al.*, Phys. Rev. Lett. **71**, 704 (1993).

⁸D. W. Rule *et al.*, *Proc. Intern. Symp. on Radiation of Relativistic Electrons in Periodical Structures*(Tomsk, 1993), p. 49.

⁹A. Potylitsin, Preprint 2/94, Nuclear Physics Institute, Tomsk, 1994.

¹⁰M. Yu. Andreyashkin *et al.*, Prib. Tekh. Eksp., No. 6, 55 (1989).

¹¹K. Yu. Amosov *et al.*, Phys. Rev. E **47**, 2207 (1993).

Translated by D. Parsons